

Final Report on

**Electro-responsive behaviour multi-wall nanotubes/gelatin composites
and cross-linked gelatin electrospun mats**

By Soo-Young Park

2007. 10

**Department of Polymer Science, Kyungpook National University, #1370 Sankyuk-
Dong, Buk-gu, Deagu 702-701, Republic of Korea.**

Tel+82-53-950-5630; Fax+82-53-590-6623; e-mail psy@knu.ac.kr

Report Documentation Page

Form Approved
OMB No. 0704-0188

Public reporting burden for the collection of information is estimated to average 1 hour per response, including the time for reviewing instructions, searching existing data sources, gathering and maintaining the data needed, and completing and reviewing the collection of information. Send comments regarding this burden estimate or any other aspect of this collection of information, including suggestions for reducing this burden, to Washington Headquarters Services, Directorate for Information Operations and Reports, 1215 Jefferson Davis Highway, Suite 1204, Arlington VA 22202-4302. Respondents should be aware that notwithstanding any other provision of law, no person shall be subject to a penalty for failing to comply with a collection of information if it does not display a currently valid OMB control number.

1. REPORT DATE

11 FEB 2008

2. REPORT TYPE

Final

3. DATES COVERED

21-02-2007 to 12-10-2007

4. TITLE AND SUBTITLE

Electro-responsive behaviour multi-wall nanotubes/gelatin composites and cross-linked gelatin electrospun mats

5a. CONTRACT NUMBER

FA48690714029

5b. GRANT NUMBER

5c. PROGRAM ELEMENT NUMBER

6. AUTHOR(S)

Soo-Yong Park

5d. PROJECT NUMBER

5e. TASK NUMBER

5f. WORK UNIT NUMBER

7. PERFORMING ORGANIZATION NAME(S) AND ADDRESS(ES)

Kyungpook National University, #1370 Sangyuk-Dong, Buk-gu, Daegu, Korea (South), NA, 702-701

8. PERFORMING ORGANIZATION REPORT NUMBER

N/A

9. SPONSORING/MONITORING AGENCY NAME(S) AND ADDRESS(ES)

AOARD, UNIT 45002, APO, AP, 96337-5002

10. SPONSOR/MONITOR'S ACRONYM(S)

AOARD

11. SPONSOR/MONITOR'S REPORT NUMBER(S)

AOARD-074029

12. DISTRIBUTION/AVAILABILITY STATEMENT

Approved for public release; distribution unlimited

13. SUPPLEMENTARY NOTES

14. ABSTRACT

Swelling, states of water, morphology, stability in the aqueous solution, and electro-mechano-chemical bending behaviors of the gelatin/chitosan blend system were studied in order to clarify the potential use of this blend system as an actuator. The gelatin/chitosan blend system was prepared in order to avoid dissolution of the pure chitosan film system in an aqueous medium and the rigidity and easy degradation of the pure gelatin system in the swollen state. The blend systems showed improved material properties: the vacuum-dried blend sample at the G75/C25 (w/w, gelatin/chitosan) ratio showed ~ 4 times swelling (in distilled water, at neutral pH and room temperature), ~ 5 times stability (in distilled water), and ~ 6 times bending (at 6V/53mm and in 0.02 M NaCl aqueous solution) as compared to pure gelatin. These enhanced properties could be explained by the introduction of free -OH, -NH₂, and -NHCOCH₃ groups of the amorphous chitosan in the blend and the network structure through the electrostatic interactions between the ammonium (-NH₃⁺) ions of the chitosan and the carboxylate (-COO⁻) ions of the gelatin. The scanning electron microscopy (SEM) micrographs of the surfaces of the blend films showed homogeneous and smooth surfaces due to the good miscibility between gelatin and chitosan. However, a different morphology from the fractured surface was found for the pure gelatin and blend systems which showed condensed and foliaceous morphologies, respectively. The leafy morphology indicates a large and homogenous pore structure, which would cause increased ion diffusion into the gel and might lead to increased bending.

15. SUBJECT TERMS

| | | | | | |
|----------------------------------|------------------------------------|-------------------------------------|--|-------------------------------------|------------------------------------|
| 16. SECURITY CLASSIFICATION OF: | | | 17. LIMITATION OF ABSTRACT Same as Report (SAR) | 18. NUMBER OF PAGES 23 | 19a. NAME OF RESPONSIBLE PERSON |
| a. REPORT unclassified | b. ABSTRACT unclassified | c. THIS PAGE unclassified | | | |

Standard Form 298 (Rev. 8-98)
Prescribed by ANSI Std Z39-18

Abstract: Swelling, states of water, morphology, stability in the aqueous solution, and electro-mechano-chemical bending behaviors of the gelatin/chitosan blend system were studied in order to clarify the potential use of this blend system as an actuator. The gelatin/chitosan blend system was prepared in order to avoid dissolution of the pure chitosan film system in an aqueous medium and the rigidity and easy degradation of the pure gelatin system in the swollen state. The blend systems showed improved material properties: the vacuum-dried blend sample at the G75/C25 (w/w, gelatin/chitosan) ratio showed ~ 4 times swelling (in distilled water, at neutral pH and room temperature), ~ 5 times stability (in distilled water), and ~ 6 times bending (at 6V/53mm and in 0.02 M NaCl aqueous solution) as compared to pure gelatin. These enhanced properties could be explained by the introduction of free -OH, -NH₂, and -NHOCOCH₃ groups of the amorphous chitosan in the blend and the network structure through the electrostatic interactions between the ammonium (-NH₃⁺) ions of the chitosan and the carboxylate (-COO⁻) ions of the gelatin. The scanning electron microscopy (SEM) micrographs of the surfaces of the blend films showed homogeneous and smooth surfaces due to the good miscibility between gelatin and chitosan. However, a different morphology from the fractured surface was found for the pure gelatin and blend systems which showed condensed and foliaceous morphologies, respectively. The leafy morphology indicates a large and homogenous pore structure, which would cause increased ion diffusion into the gel and might lead to increased bending.

Introduction

Recently interest is growing in the development of artificial muscle-like actuators. An actuator is an energy transducer that can convert a variety of forms of energy into mechanical quantities such as displacement, strain, velocity, and stress. Various materials have been used for the development of actuators, including shape-memory alloys and electrostrictive and piezoelectric materials ¹. However, for the materials to have muscle-like movements, they should be soft and deformable in response to external stimuli such as changes in the electric field or temperature. Polymeric materials such as polymer gels ²⁻³, conducting polymers ⁴⁻⁵, carbon nanotube composites ⁶⁻⁸, and dielectric elastomers ⁹ are some of the most promising materials for artificial muscles because of their advantageous properties, such as high processability, softness, high corrosion resistance, low manufacturing costs, and operation compliance ². Among these materials, polymer gels have attracted much attention because of the fluids they contain in their three-dimensional network structures, which provide softness as well as high biocompatibility. Polymer gels undergo reversible transformation through dramatic swelling and shrinking upon exposure and removal of stimuli such as temperature ¹⁰⁻¹², pH ¹³, solvent composition, ionic strength ¹⁴⁻¹⁵, and magnetic and electric fields ¹⁶⁻¹⁷. Amongst these possibilities, an electric field is of most interest, in view of the high sensitivity of gels to an electric field and the large amount of mechanical energy produced upon exposure ¹.

Gelatin is a high molecular weight polypeptide obtained by the controlled hydrolysis of collagen ¹⁸. The major amino acids in gelatin are glycine (30%) and

proline/hydroxyproline (25%), where frequently occurring sequences are -glycine-X-proline, -glycine-proline-X and -glycine-X-hydroxyproline, where X may be any amino acid ¹⁹. Gelatin is a good film and particle forming material ²⁰ with uses in medicine such as in plasma expanders, wound dressings, adhesives, and controlled drug delivery ^{21, 22}. However, gelatin has also limitations in practical applications owing to its weak mechanical strength and degradation in vivo ²³. Chitosan (produced by alkaline N-deacetylation of chitin ²⁴) is a poly-amino-saccharid and one of the cationic natural functional biopolymers with a repeating structural unit of 2-acetomido-2-deoxy- β -D-glucose. Chitosan offers special characteristics, such as biocompatibility, hydrophilicity, bioactivity, non-antigenicity, and non-toxicity (its degradation products are natural metabolites) ²⁵. Apart from all these advantages, chitosan has a limitation of being instable in an aqueous medium, due to the salt formation between ammonium ($-\text{NH}_3^+$) ions along the chitosan chains and the carboxylate ($-\text{COO}^-$) ions of the acetic acid, which is the solvent of chitosan. The blending of gelatin and chitosan may prove to be advantageous, as gelatin and chitosan are natural and biocompatible polyelectrolytes which may react in the blend systems to form a polyelectrolytic complex *via* interactions of ammonium ($-\text{NH}_3^+$) ions of the chitosan and carboxylate ($-\text{COO}^-$) ions of the gelatin.

In continuation of our previous efforts to improve the electro-mechano-chemical behavior of the gelatin ²⁶, we developed a gelatin/chitosan blend system in order to overcome the shortcomings of the complete dissolution of chitosan film in an aqueous medium, and the rigidity and easy degradation of gelatin in the swollen state. In this paper, swelling, states of water, morphologies, stability and electro-mechano-chemical bending behaviors of the blend films will be reported.

Experimental

Materials

Gelatin (Type B, bovine skin) and NaCl (reagent grade, purity 99%) were purchased from Sigma Aldrich (Steinheim, Germany). Urea, sodium hydroxide, and acetic acid were acquired from Sigma, Fluka (Buche Switzland), and Duksan, respectively, and were used without further purification. Chitosan was prepared by the deacetylation of 10 wt % chitin (red crab) of East Sea of Korea (acquired from the Dongbo Chemical Co - Sekcho, Korea) in a 50 wt % NaOH alkali water solution at 110 °C for 4 h. The solid portion was filtered and washed thoroughly with distilled water until it became a nearly neutral pH. It was dried in a vacuum at room temperature, finely cut in a knife-milling machine, and sieved through a 60-mesh screen (pore size, 250µm). The degree of deacetylation and the viscosity average molecular weight was calculated according to the reported methods²⁷⁻²⁸. The chitosan used is summarized in Table 1.

Table 1. Characteristics of the chitin and chitosan used in this study.

| Sample | Chitin | Chitosan |
|---|---------|----------|
| Degree of deacetylation (%) ²⁷ | 65.7 | 86.7 |
| Viscosity-averaged molecular weight (¹ M _v) ²⁹ | 550,000 | 112,000 |
| Ash content (%) ²⁹ | 1.0 (↓) | 0.5 (↓) |
| Protein content (wt %) ²⁹ | 1.0 (↓) | 0.5 (↓) |

¹M_v is viscosity-averaged molecular weight calculated using $[\eta] = k.M_v^\alpha$ with k and α of 8.93×10^{-4} and 0.71, respectively.

Preparation of the blend film

Chitosan was dissolved in a 0.2 M aqueous acetic acid solution and gelatin was dissolved in deionized water at above 45 °C using a water bath. The concentrations of chitosan and the gelatin were 40 and 80 g/L, respectively. The two solutions were mixed for two hours at 45 °C to get a homogeneous blend solution, poured onto a glass Petri dish for film casting, and allowed to dry at room temperature. The dried films were removed from the Petri dish and further dried in a vacuum oven at 60 °C until constant weight was achieved. The blend ratio (w/w, gelatin/chitosan) in this paper is expressed as GXXCYY, where XX and YY represent the weights of gelatin and chitosan, respectively.

Degree of Swelling

Rectangular samples of the pure gelatin and blend system ($16 \times 15 \times \sim 0.18 \text{ mm}^3$) were prepared for swelling experiment. The prepared samples were thoroughly dried under vacuum at 60 °C until constant weight was achieved. The samples were immersed in a vial containing 15 mL of the deionized water at neutral pH and room temperature. Each sample was taken out of the vial at regular intervals, wiped between filter papers to remove the excess surface water, and then weighed. The degree of swelling was calculated as follow,

$$\text{Swelling ratio (\%)} = \frac{(W_o - W)}{W} \times 100 \text{----- (1)}^{30}$$

where W_o and W are the weights of the swollen and dried samples, respectively.

Measurement of bound and unbound waters

States of water in the hydrogel samples were determined by differential scanning calorimetry (DSC) using a DuPont 2000 Thermal Analyzer ³¹. Each sample was immersed in a vial containing 15 mL of the deionized water and allowed to swell until equilibrium. The sealed pan was quickly frozen to -40 °C, left to equilibrate for several minutes, and then heated to 40 °C at a scanning speed of 5 °C/min with flow of nitrogen. The sample pan was removed from the DSC, dried at 105 °C for 24 hrs, and then weighed. The total amount of water was calculated by subtracting the weight of the dried sample pan from the total weight of the initial sample pan. The amounts of unbound and bound water were determined from the melting enthalpies as follow,

$$W_b(\%) = W_t - (W_{ub}) = W_t - \left(\frac{Q_{endo}}{Q_f}\right) \times 100 \text{-----} (2)^{30}$$

where W_t , W_b , and W_{ub} , are the amounts of the total, bound and unbound waters, respectively, and Q_{endo} and Q_f are the measured heat of fusion from DSC and the heat of fusion of ice (79.9 cal/g), respectively.

Morphology

Scanning electron microscopy (SEM) of the freeze-dried films was performed using a Hitachi 570. The freeze-dried samples ($16 \times 15 \times \sim 0.18 \text{ mm}^3$) were prepared by swelling them to equilibrium in deionized water, blotting with filter paper to remove the surface water, freezing in a freezer (IISHIN DF9007) at -70 °C for 30 min, and drying in

a drying chamber (IISHIN FD5505) in the frozen state at -54 °C for 16 hours. The prepared samples were then fractured in liquid nitrogen, fixed on the brass holder, and coated with platinum for SEM.

Stability in water

The degree of stability in aqueous solution was examined at neutral pH and room temperature. The air-dried films were weighed, immersed in the vial with an aqueous solution, taken out from the vial at intervals of one to five days, dried for 48 hrs in a hood, and weighed again. The degree of stability of the films in the aqueous medium was expressed as follow,

$$S (\%) = \frac{W_2}{W_1} \times 100 \text{-----} (3)^{32}$$

where W_1 and W_2 are the weights of dried films before and after the experiment, respectively.

Electro-mechano-chemical Behavior

Electro-mechano-chemical behavior was studied under a DC electric field. The samples ($30 \times 5 \times 0.25 \text{ mm}^3$) were fixed at the top of a glass beaker (cantilever type) containing 0.02 M NaCl aqueous solution, in which there were two parallel platinum electrodes ($50 \times 10 \times 0.31 \text{ mm}^3$) 52 mm apart. The deformation was recorded with a digital camera at a fixed position and focus, and the bending was expressed as the ratio of

x to y , where x and y are the x - y coordinates of the free end of the film^{26,33}, as shown in Figure 1.

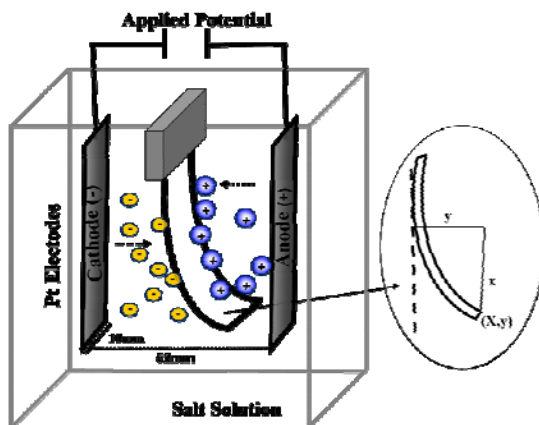


Figure 1. Experimental apparatus for the electro-mechano-chemical characterization of the hydrogel.

Results and discussion

Figure 2 shows FT-IR spectra of the gelatin, chitosan, and the blend (G67C33). Pure gelatin (Figure 2a) shows a broad strong peak at 1650 cm^{-1} , which corresponds to C=O stretching of the carboxylic acid. Pure chitosan (Figure 2b) shows a strong peak at 1680 cm^{-1} , a shoulder at 1630 cm^{-1} and a peak at 1538 cm^{-1} which correspond to C=O stretching of the N-acetyl group, scissor vibration of the amine group and ammonium ($-\text{NH}_3^+$) ions, respectively. The G67C33 blend (Figure 2c) shows double peaks at 1680 and 1630 cm^{-1} ³⁴, and a peak at 1538 cm^{-1} with reduced relative intensities at 1680 and 1538 cm^{-1} as compared to that at 1630 cm^{-1} , whereas the peak at 1650 cm^{-1} no longer exists. This might be due to some degree of amidization between the ammonium ($-\text{NH}_3^+$)

ions of the chitosan and the carboxylate (COO^-) ions of the gelatin by the partial conversion of electrostatic bonds into chemical bonds (condensation reaction) as discussed by Bernable et al ³⁵.

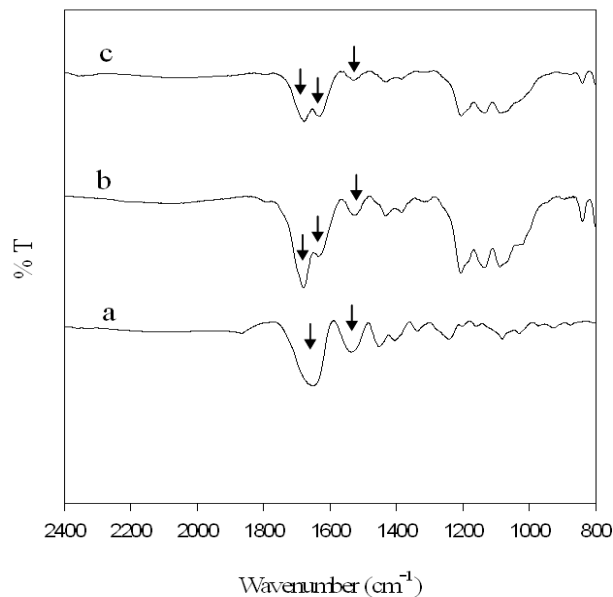


Figure 2. FT-IR spectra of (a) gelatin, (b) chitosan and (c) G67C33; arrows showing the peaks are discussed in text.

Figure 3a shows the degree of swelling as a function of time, calculated using Eq. (1) and three independent trials were averaged. The samples reached equilibrium after ~ 4 hrs and the equilibrium values were plotted as a function of the blend ratio in Figure 3b. The equilibrium swelling has a maximum at G75C25. The swelling would increase by the introduction of free $-\text{OH}$, $-\text{HN}_2$, and $-\text{NHOCOCH}_3$ groups as the chitosan content increases in the blend ²⁸. However, the increase in chitosan content would also generate the network structure (through the electrostatic interaction between the ammonium ($-\text{NH}_3^+$) ions of the chitosan and the carboxylate ($-\text{COO}^-$) ions of the gelatin) which causes

decrease in swelling due to stiffness of complexed chains. This combination of opposite effects might produce a maximum at G75C25. Interestingly, the degree of swelling at G75C25 is almost 5000 %, which is ~ 4 times that of pure gelatin (~ 800%). This large increase indicates that this blend system has much potential for better electro-mechano-chemical behavior (as discussed later).

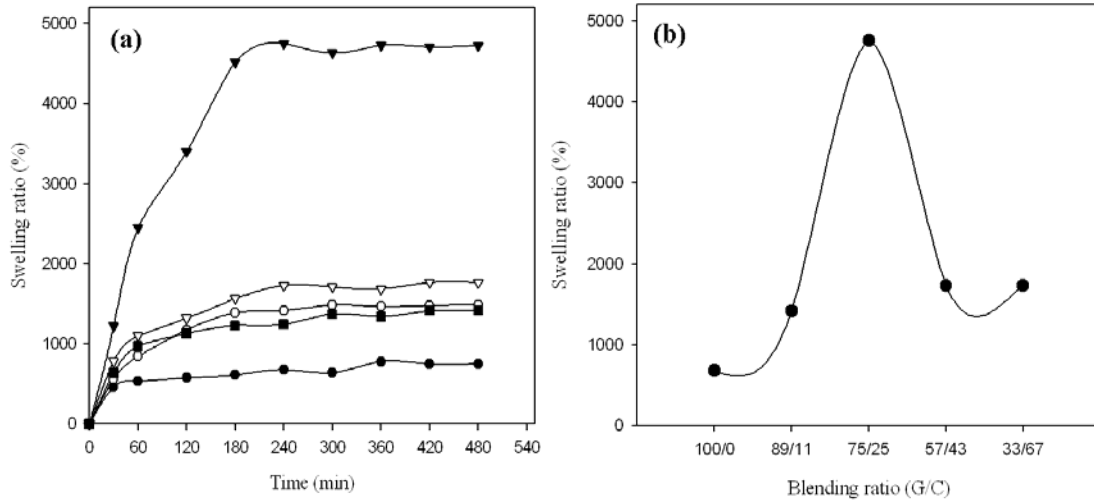


Figure 3. (a) Swelling ratio in the aqueous solution as a function of time; (●) G100C00, (○) G89C11, (▼) G75C25, (△) G57C43 and (■) G33C67; (b) equilibrium swelling ratio against blend ratios.

The kinetics of the swelling can be described by the following second order rate equations³⁶,

$$\frac{dW}{dt} = k(W_{\infty} - W)^2 \dots\dots\dots (4)$$

$$\frac{t}{W} = A + Bt \dots\dots\dots (5)$$

where k , W_∞ , W are the rate constant, the maximum (equilibrium) solvent uptake, and the amount of the solvent absorbed (per gram of gelatin) at time t , respectively, and $(W_\infty - W)$ is the swelling capacity. $A (=1/K_\infty^2)$ and $B (=1/W_\infty)$ are the intercept and slope of the t/W vs. t plot, respectively. Eq. (5) follows from the integration and rearrangement of Eq. (4).

Figure 4 shows the linear regression results of the t/W vs. t plot and the resulting constants A and B are given in Table 2. The straight lines in Figure 4 indicate that the blend system indeed follows second-order kinetics, where the rate of swelling at any time is directly proportional to the square of the swelling capacity. Note that similar to the equilibrium swelling, both K_∞ (rate of swelling) and W_∞ have maximums at G75C25 (see Table 2).

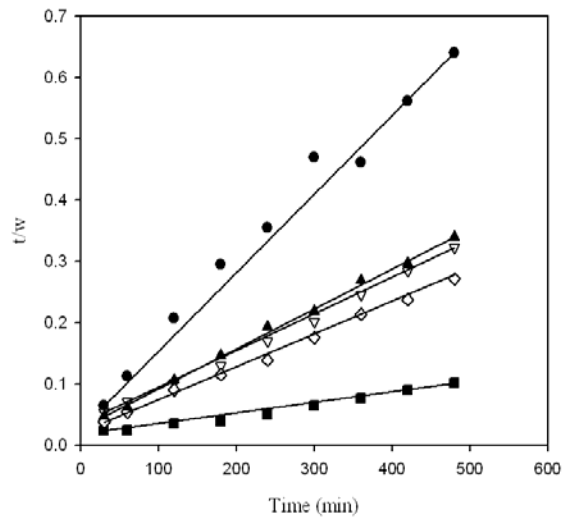


Figure 4. Linear regression of the swelling curves (Figure 3); (●) G100C00, (○) G89C11, (■) G75C25, (□) G57C43 and (▲) G33C67 using Eq. (5).

Table 2. Linear regression results of Figure 4 using Eq. (5).

| Sample | A (min/W ¹) | B (1/W) | K _∞ (√(W/min)) | W _∞ (W) |
|---------|----------------------------|------------|------------------------------|-----------------------|
| G100C00 | 0.04979 | 0.00124 | 4.4816 | 806 |
| G89C11 | 0.03033 | 5.97E-04 | 5.7420 | 1675 |
| G75C25 | 0.01348 | 1.97 E-04 | 8.6130 | 5057 |
| G57C43 | 0.02340 | 5.14 E-04 | 6.5372 | 1945 |
| G33C67 | 0.02750 | 6.54 E-04 | 6.0302 | 1529 |

¹W is the percentage of the amount of the solvent absorbed (per gram of gelatin)

Figure 5 shows the DSC thermograms for the swollen samples. There are three types of waters in hydrogel ³¹, such as unbound (freezing), intermediate (freezing-bound) and bound (nonfreezing). Unbound (freezing) water does not form hydrogen bonds with the polymer molecules and shows a melting endotherm in DSC, while bound (nonfreezing) water forms hydrogen-bonds and shows no melting endotherm in DSC. Intermediate (freezing-bound) water interacts with the polymer molecules but shows a melting endotherm. The endotherm at ~ 0 °C represents the amount of the combined unbound and intermediate (freezing-bound) waters. Thus, the amount of unbound water in Eq. (2) includes the intermediate (freezing-bond) water. The amounts of the different states of water were calculated using Eq. (2) and listed in Table 3. Similar to the equilibrium swelling and the kinetics, the unbound water (including intermediate water) has a maximum at G75C25. In contrast, the bounded water did not change much, likely due to the nearly constant contact area that is maintained between water and blend film by changing the blend ratio. The melting temperatures were a little bit higher than 0 °C.

The slight shift in the melting temperature of the ice was reported for the melting of the interior of the ice crystal³⁷.

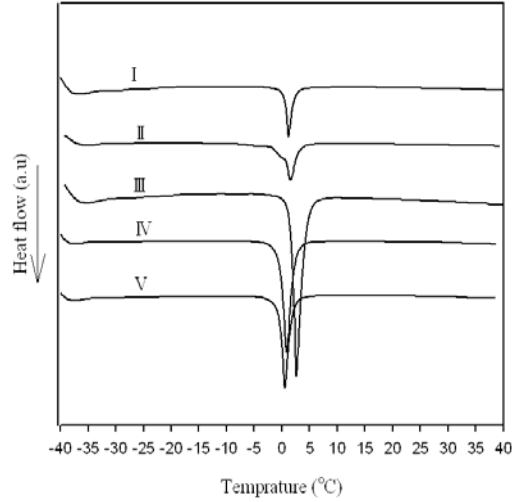


Figure 5. DSC thermograms of the swollen gel samples of (I) G100C00, (II) G89C11, (III) G75C25, (IV) G57C43, and (V) G33C67.

Table 3. The amounts of the different states of water in the hydrogels calculated using Eq. (2).

| Sample | W_f (%) | W_{ub} (%) | W_b (%) |
|---------|--------------|-----------------|--------------|
| G100C00 | 80.93 | 19.25 | 61.68 |
| G89C11 | 84.90 | 20.98 | 63.92 |
| G75C25 | 95.30 | 31.85 | 63.45 |

| | | | |
|--------|-------|-------|-------|
| G57C43 | 88.92 | 23.19 | 65.73 |
| G33C67 | 85.14 | 24.61 | 60.53 |

Morphology

Figure 6 shows the SEM micrographs of the freeze-dried films. The surfaces of the films (Figure 6a - e) are almost closed, homogeneous, and smooth with no porosity except for G75C25 and gelatin, which are foliaceous and exhibit small craters, respectively. The homogeneous and smooth surface might be due to the good miscibility between gelatin and chitosan³⁸⁻³⁹. The fractured surfaces of the films (Figure 6f - j) show open structure (foliaceous morphology) except for the pure gelatin film (Figure 6f), which has condensed structure with small pores and thick walls. The most open structure was observed for G75C25, which might be due to increased swelling as earlier discussed. The open leafy structure might result in a higher ionic gradient that induces more bending in an electro-mechano-chemical experiment due to the easy diffusion of ions through an open structure⁴⁰⁻⁴¹.

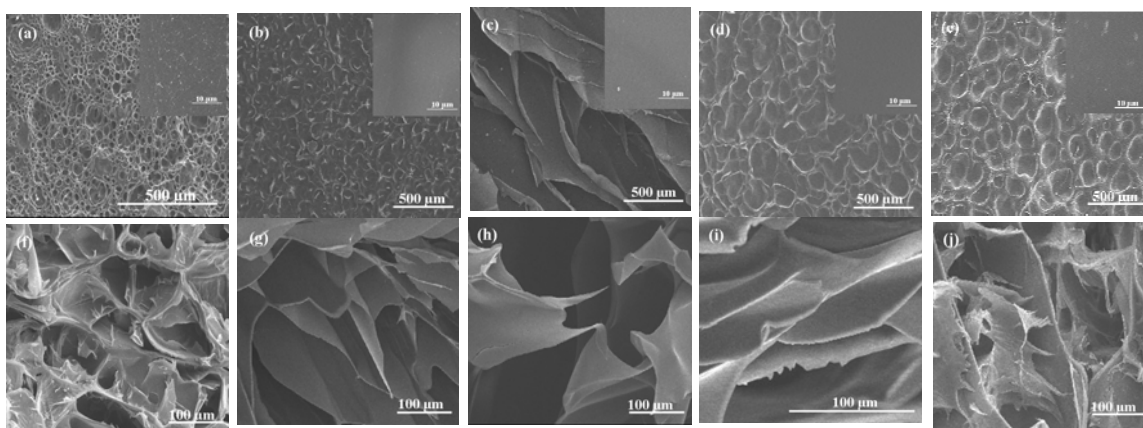


Figure 6. SEM micrographs of the blend freeze-dried samples; the surface images of (a) G100C00 (b) G89C11 (c) G75C25 and (d) G57C43 and (e) G33C67 and the fractured surfaces of (f) G100C00, (g) G89C11 (h) G75C25 (i) G57C43 and (j) G33C67.

Stability study

Figure 7 shows the degree of stability (Eq. (3)) in an aqueous solution at neutral pH. The remained weight of G75C25 was more than 90 % for the first 5 days, although that of the pure gelatin was ~ 60 % for the first day and dropped to ~ 45 % after 5 days. This stability of G75C25 may be due to the strong network structure, as earlier discussed.

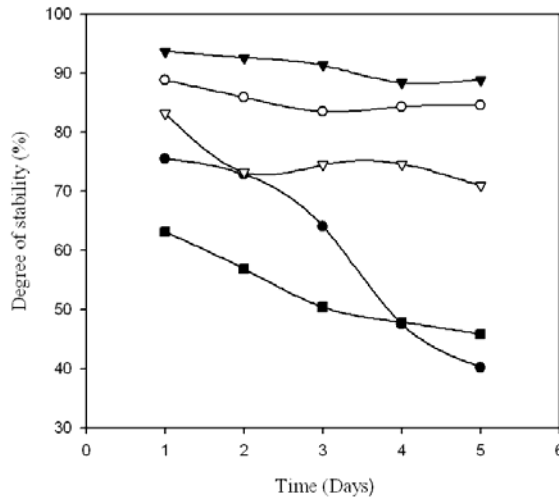


Figure 7. The degree of stability (Eq. (3)) of the (●) G100C00, (○) G89C11, (▼) G75C25, () G57C43 and (■) G33C67 films in aqueous solution at neutral pH.

Electro-mechano-chemical behavior

Figure 8 shows the electro-mechano-chemical behavior of the gelatin hydrogel. Figures 8a and b show the two-stage bending phenomena, where the initial bending

toward the anode changes direction toward the cathode under the applied DC current after some time. Figures 8c - e show the models of the initial and final movements of the hydrogels. The bending of the hydrogel is mainly due to the osmotic pressure difference between the anode and cathode sides of the film, i.e. $\Delta \pi = \pi_1 - \pi_2$ where π_1 and π_2 are the osmotic pressures at the anode and cathode sides, respectively. Initially, a large amount of positive ions will be deposited on the anode surface of the film resulting in higher π_2 as compared to π_1 ; the large sodium (Na^+) ions are difficult to penetrate in the film but chloride (Cl^-) ions are easy and fast to penetrate in the film. The higher π_2 (at the cathode side) would cause more water to penetrate into the gel at the cathode side, which would cause the hydrogel to bend towards the anode (Figure 8c). The accumulated sodium (Na^+) ions were then diffused into the gel after some time. This diffusion of the sodium (Na^+) ions in the hydrogel film might decrease ionic concentration at the anode-side inside gel film and lead to an increase in π_1 , and the bending towards the cathode³³ (Figure 8d). However, in contrast to the pure gelatin hydrogel, the blend samples did not show a two-stage bending but a bending only towards the anode (Figure 8e), which may be attributed to the increase in the fixed ammonium ($-\text{NH}_3^+$) ions in the blend which would give cationic character to the gel⁴². The ammonium ($-\text{NH}_3^+$) ions not only reduce the diffusion of positive ions in the gel film (shielding) due to possible repulsive forces between the similar charged ammonium ($-\text{NH}_3^+$) ions and counter sodium (Na^+) ions, but also create increased osmotic pressure (mass movement of the chloride (Cl^-) ions) at the cathode due to likeness of the opposite charged ammonium ($-\text{NH}_3^+$) and chloride (Cl^-) ions, respectively.

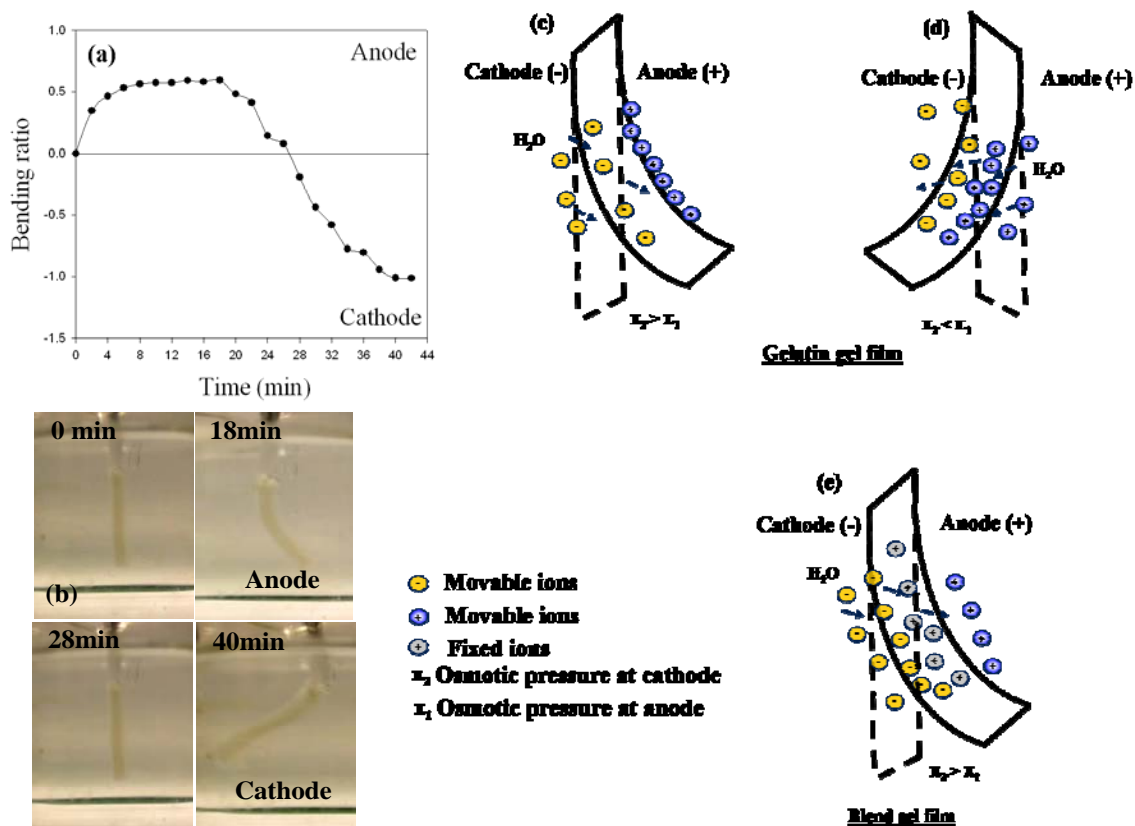


Figure 8. (a) Bending behavior of the G100C00 film with the dimension of $30 \times 5 \times 0.25$ mm³ in a 0.02 M NaCl aqueous solution and at a 6V/52mm applied electric field, (b) digital camera images of the bending, and (c, d and e) illustrations of the proposed osmotic pressure based on bending mechanism.

Figure 9a shows the electro-mechano-chemical bending curves at a 6V/52mm applied electric field. The bending showed a maximum at G75C25, in agreement with the swelling and morphological results. The bending of all studied samples reached equilibrium after ~ 8 minutes. The equilibrium bending of G75C25 (~3) was ~ 6 times higher than that of the pure gelatin (~ 0.5). Figure 9b shows the electro-mechano-

chemical bending curves at 9V/52mm. The bending ratio as well as the rate of bending increases with increase in electric potential, indicating that the increase in the electric potential might increase the osmotic pressure as well as the rate of the diffusion of the ions. Figure 9c illustrates the bending of G75C25 in 0.02 M NaCl solution with an alternating on (6V/52mm) and off (0V/52mm) electric field. Good stimuli behavior was observed according to the applied electric potential which signifies the effectiveness of the gelatin/chitosan blend system for the electro-mechano-chemical bending.

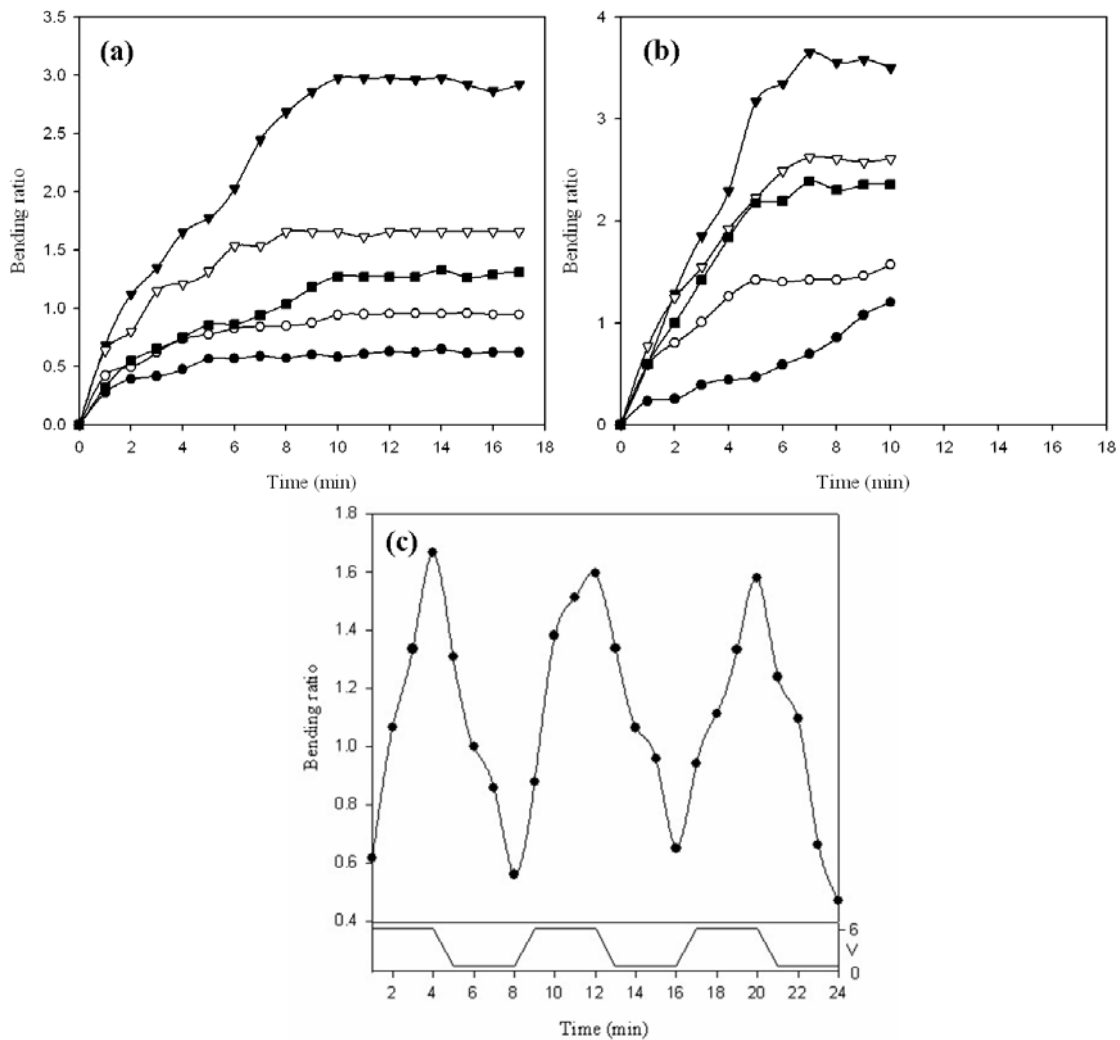


Figure 9. Time courses for bending (toward the anode) of (●)G100C00, (○) G89C11, (▼) G75C25, () G57C43 and (■) G33C67 (wet state) gel films with the dimension of $30 \times 5 \times 0.25 \text{ mm}^3$ at (a) 6V/52mm and (b) 9V/52mm applied electric field; (c) on-and-off bending behavior of G75C25 at 6V/52mm.

Conclusions

The gelatin/chitosan blend system was prepared in order to overcome the undesirable properties of chitosan film (which is dissolvable in aqueous medium) and the gelatin (which is rigid and easily degraded in the swollen state) and to clarify the potential of the blend systems as an actuator. The blends showed improved material properties: the vacuum-dried blend sample at the G75C25 (w/w, gelatin/chitosan) ratio showed ~ 4 times swelling (in distilled water, at neutral pH and room temperature), ~ 5 times stability (in distilled water), and ~ 6 times bending (at 6V/52mm) as compared to pure gelatin. These improved properties might be due to the introduction of free -OH, -NH₂, and -NHOCOCH₃ groups of the amorphous chitosan in the blend and the network structure through the electrostatic interactions between the ammonium (-NH₃⁺) ions of the chitosan and the carboxylate (-COO⁻) ions of the gelatin. The foliaceous morphology, as observed from the freeze-dried sample, could explain large swelling in blend samples which might enhance ions diffusion and lead to an increase of bending.

References

- [1] T. Ikeda, J. Mamiya and Y. Yu, *Angew. Chem. Int. Ed.*, 2007, **46**, 506 - 528.
- [2] Y. Yu and T. Ikeda, *Angew. Chem. Int. Ed.*, 2006, **45**, 5416 - 5418.
- [3] Y. Osada, H. Okuzaki and H. Hori, *Nature*, 1992, **355**, 242 - 244.
- [4] E. Smela, *Adv. Mater.*, 2003, **15**, 481- 494.
- [5] W. Lu, A. G. Fadeev, B. Qi, E. Smela, B. R. Mattes, J. Ding, G. M. Spinks, J. Mazurkiewicz, D. Zhou, G. G. Wallace, D. R. MacFarlane, S. A. Forsyth and M. Forsyth, *Science*, 2002, **297**, 983 - 987.
- [6] R. H. Baughman, C. Cui, A. A. Zakhidov, Z. Iqbal, J. N. Barisci, G. M. Spinks, G. G. Wallace, A. Mazzoldi, D. De Rossi, A. G. Rinzler, O. Jaschinski, S. Roth and M. Kertesz, *Science*, 1999, **284**, 1340 - 1344.
- [7] P. Kim and C. M. Lieber, *Science*, 1999, **286**, 2148 - 2150.
- [8] Y. Zhang and S. Iijima, *Phys. Rev. Lett.*, 1999, **82**, 3472 - 3475.
- [9] R. Pelrine, R. Kornbluh, Q. Pei and J. Joseph, *Science*, 2000, **287**, 836 - 839.
- [10] T. Okano, Y. H. Bae, H. Jacobs and S. W. Kim, *J. Control. Release*, 1990, **11** 255 - 265.
- [11] H. G. Shield, *Prog. Polym. Sci.*, 1992, **17**, 163 - 249.

- [12] H. M. Zareie, E. V. Bulmus, A. P. Gunning, A. S. Hoffman, E. Piskin and V. J. Morris, *Polym.*, 2000, **41**, 6723 - 6727.
- [13] T. G. Park and A. S. Hoffman, *J. Appl. Polym. Sci.*, 1992, **46**, 659 - 671.
- [14] S.Y. Kim, H. S. Shin, Y. M. Lee and C. N. Jeong, *J. Appl. Polym. Sci.*, 1999, **73**, 1675 - 1683.
- [15] S. J. Kim, K. J. Lee, S. I. Kim, Y. M. Lee, T. D. Chung and S. H. Lee, *J. Appl. Polym. Sci.*, 2003, **89**, 2301 - 2305.
- [16] S. Kaewpirom and S. Boonsang, *Eur. Polym. J.*, 2006, **42**, 1609 - 1616.
- [17] E. A. Moschou, M. J. Madou, L. G. Bachas and S. Duanert, *Sensor Actuat. B-Chem.*, 2006, **115**, 379 - 383.
- [18] S. B. Ross-Murphy, *Polym.*, 1992, **33**, 2622 - 2627.
- [19] B. Pinto-Iguanero, A. Olivares-Perez, A. W. Mendez-Alvarado, I. Fuentes-Tapia and C. G. Trevino-Palacios, *Opt. Mater.*, 2003, **22**, 397 - 404.
- [20] X. J. Yang, P. J. Zheng, Z. D. Cui, N. Q. Zhao, Y. F. Wang and K. D. Yao, *Polym. Int.*, 1997, **44**, 448 - 452.
- [21] J. P. Draye, B. Delaey, A. Van de Voorde, A. Van Den Bulcke, B. De Reu and E. Schacht, *Biomaterials*, 1998, **19**, 1677 - 1687.
- [22] E. Schach, A. Van Den Bulcke, B. Bogdanov, J. P. Draye and B. Delaey, *Polym. Mater. Sci. Eng.*, 1998, **79**, 222 - 223.

- [23] Y. Z. Wan, Y. L. Wang, K. D. Yao and G.. X. Cheng, *J. Appl. Polym. Sci.* 2000, **75**, 994 - 998.
- [24] K. C. Gupta and M. N. V. Ravi Kumar, *Polym. Int.*, 2000, **49**, 141 – 146.
- [25] S. J. Kim, S. G. Yoon, K. B. Lee, Y. D. Park and S. I. Kim, *Solid State Ionics*, 2003, **164**, 199 - 204.
- [26] S. Haider, S. Y. Park, K. Saeed and B. L. Farmer, *Sensor Actuat. B-Chem.*, 2007, **124**, 517 - 528.
- [27] M. Miya, R. Iwamoto, S. Yoshikawa and S. Mima, *Int. J. Biol. Macromol.*, 1980, **2**, 323 - 324.
- [28] S. H. Lee, S. Y. Park and J. H. Choi, *Appl. Polym. Sci.*, 2004, **92**, 2054 - 2062.
- [29] S. H. Lee, S. M. Park and Y. Kim, *Carbohydr. Polym.*, 2007, **70**, 53 - 60.
- [30] S. J. Kim, S. J. Park and S. I. Kim, *Smart Mater. Struct.*, 2004, **13**, 317 - 322.
- [31] A. B. Mansor and H. B. Malcolm, *Poly. Int.*, 1994, **33**, 273 - 277.
- [32] P. Snagsanoh and P. Supaphol, *Bioacromolecules*, 2006, **7**, 2710 - 2714.
- [33] M. Homma, Y. Seid and Y. Nakano, *Appl. Polym. Sci.*, 2001, **82**, 76 - 80.
- [34] G. Socrates, *Infrared and Raman characteristics group frequencies table and charts*, West Sussex, John Wiley& Sons Ltd UK, 3rd edn., 2001, pp. 143.
- [35] P. Bernable, C. Peniche and W. A. Monal, *Polym. Bull.*, 2005, **55**, 367 - 375.
- [36] I. Katime, J. L. Velada, R. Novoa, and E. Diaz de Apodaca, *Polym. Int.*, 1996, **40**, 281 - 286.
- [37] H. Iglev, M. Schmeisser, K. Simeonidis, A. Thaller and A. Laubereau, *Nature*, 2006, **439**, 183 - 186.
- [38] C. Lingyun, D. Yumin and H. Ronghua, *Polym. Int.*, 2003, **52**, 56 - 61.

- [39] M. R. Guilherme, G. M. Campese, E. Radovanovic, A. F. Rubira, J. P. A. Feitosa and E. C. Muniz, *Polym.*, 2005, **46**, 7867 - 7873.
- [40] S. G. Yoon, I. Y. Kim, S. I. Kim and S. J. Kim, *Polym. Int.*, 2005, **54**, 1169 - 1174.
- [41] S. Sun and A. F. T. Mark, *J. Polym. Sci. Pol. Phys.*, 2000, **39**, 236 - 246.
- [42] T. Shiga and T. Kurauchi, *J. Appl. Polym. Sci.*, 1990, **39**, 2305 - 2320.